Colloquia: IWM-EC 2021

Highlights from CHIMERA Collaboration

E. Geraci[1][2][*], L. Acosta[3], G. Cardella[2], A. Castoldi[4],
E. De Filippo[2], B. Gnoffo[1][2], C. Guazzoni[4], G. Lanzalone[5][6],
C. Maiolino[6], N. S. Martorana[1][6], A. Pagano[2], E. V. Pagano[6],
M. Papa[2], S. Pirrone[2], G. Politi[1][2], F. Risitano[2][7], F. Rizzo[1][6],
P. Russotto[6], V. Sicari[4], A. Trifiró[2][7] and M. Trimarchi[2][7]

[1] *Dipartimento di Fisica e Astronomia "Ettore Majorana", Università degli Studi di Catania Catania, Italy*
[2] *INFN, Sezione di Catania - Catania, Italy*
[3] *Instituto de Fìsica, Universidad Nacional Autònoma de México - Mexico City, Mexico*
[4] *DEIB Politecnico Milano and INFN, Sezione di Milano - Milano, Italy*
[5] *Università degli Studi di Enna KORE - Enna, Italy*
[6] *INFN-LNS - Catania, Italy*
[7] *Dipartimento MIFT, Università degli Studi di Messina - Messina, Italy*

received 12 May 2022

Summary. — The activities performed by the CHIMERA Collaboration since the 2018 IWM-EC workshop are outlined in this paper. Experiments performed in the last three years and results obtained through dedicated analyses of experimental data already acquired are summarized. A brief report on the activities conducted at GSI is also included.

1. – Introduction

The Covid-19 pandemic situation provoked severe plan changes in CHIMERA's experimental programs and in its daily activities. Some of the experiments planned for the first semester of 2020 had to be postponed and the pause imposed to the operation of accelerators in September 2020, due to the POTLNS project, forced some of the experiments to be rescheduled for the future, once the LNS facilities will be fully operational again. Sophisticated analyses were performed on accumulated experimental data and some results are briefly reported hereafter, whereas more detailed presentations are included in different contributions to the present volume.

(*) E-mail: elena.geraci@ct.infn.it

2. – Exploring symmetry energy at high density

In the last decade, CHIMERA Collaboration investigated the symmetry energy at supra saturation densities, by means of experimental campaigns performed at GSI. In particular, a first experiment was realized in 2011 with a complex experimental array, including several experimental apparata, such as Land, used to detect neutrons and light charged particles, the Aladin ToF Wall, four rings of CHIMERA multi-detector and four rings of Microball Array, arranged to measure the orientation of the reaction plane and to study the event characterization [1]. Collisions of $Au + Au$ were studied at $400 \, AMeV$, and the comparison of the elliptic-flow ratio of neutrons with respect to charged particles with UrQMD predictions [2] allowed obtaining constraints on the symmetry energy, which supported a moderately soft to linear density dependence of the potential part in the parametrization of the symmetry energy. A $\gamma = 0.72 \pm 0.19$, corresponding to a slope parameter $L = 72 \pm 13 \, MeV$, was obtained. The elliptic flow, developed in relativistic heavy ion collisions, has been proven, theoretically and experimentally, to have a unique sensitivity and robustness in probing the symmetry energy above the saturation density. A new experiment has been recently planned with the purpose of exploring higher energies and tightening constraints of the symmetry energy at densities around $2 \, \rho_0$; the experiment proposal (ASY-EOS II) has been submitted to the GSI PAC [3]; it received positive comments and hopefully it will be realized by the end of 2024. Au beams at 250, 400, 600, 1000 AMeV were proposed to be used to simultaneously extract neutrons and protons elliptic flow, excitation function of the neutron/proton elliptic flow ratio, yields and ratios, energy and angular distributions, correlation functions for neutron, protons and isotopically resolved light clusters. The experimental set-up, shown in fig. 1, will be based on 4 double rings of CHIMERA, devoted to the detection, in charge and energy, of light clusters and light charged particles that allow, together with the R3B New Time-of-Flight Wall TOF, the determination of the centrality of the collisions and the orientation of the reaction plane at polar angles up to $30°$. The presence of KRAB (KRAkow Barrel) detector [4] will provide a fast multiplicity trigger signal as well as precise azimuthal distributions for charged particles beyond the angular acceptance of the CHIMERA+TOFD set-up. Twelve double planes of Neuland [5] will measure neutron, p, d, t, light charged particles and accordingly the n/p ratio emitted from mid-rapidity; in particular, the well resolved proton spectra will allow efficiently probing densities about 30% higher than densities with only elemental resolution. The KRATTA triple telescopes and the FARCOS [6] array will be placed near the target for measuring light charged particles and clusters at mid-rapidity and at backward angles, respectively, which can provide key information for advanced tuning of clusterization algorithms used in transport models.

Meanwhile, several members of CHIMERA Collaboration joined the R3B (Reactions with Relativistic Radioactive Beams) collaboration [7], and participated to several experiments performed at GSI, mainly working with Neuland apparatus. NeuLAND (New Large-Area Neutron Detector) [5] is a next-generation neutron detector designed for the R3B experiment at FAIR (Facility for Antiproton and Ion Research). NeuLAND detects neutrons with energies from 100 to 1000 MeV, featuring a high detection efficiency, a high spatial and time resolution, and a large multi-neutron reconstruction efficiency. It is composed of organic scintillators bars, 2.5 meter long arranged on 30 double planes, read by photomultipliers. Twelve planes are already operating and are used in experiments exploring fission of unstable nuclei, evolution of the collective response as a function of isospin and the dipole strength of exotic nuclei, relevant to nuclear astrophysics,
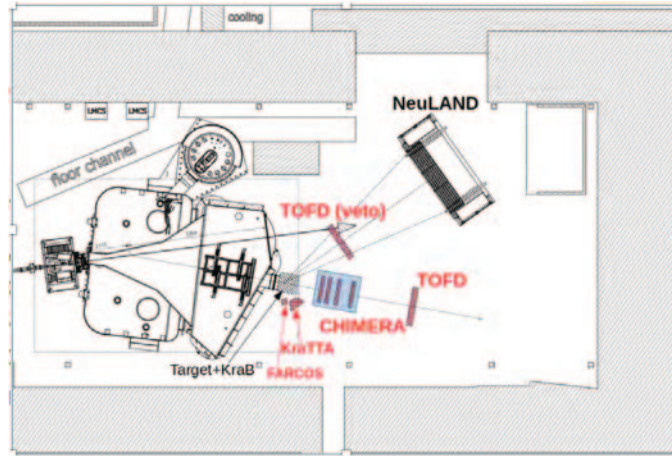
Fig. 1. – Scale drawing of the proposed set-up for the ASY-EOS II experiment to be realized at GSI (Darmstadt, Germany).

multifragmentation and the influence of the isospin degree of freedom, and investigations of flow and the nuclear equation of state.

3. – Study of dynamical contributions at Fermi Energies

In the last three years, several experiments were performed at LNS with CHIMERA and FARCOS multi-detectors, aimed at the study of the competition between different reaction mechanisms and the influence of the isospin degree of freedom. In particular, the coexistence of dynamical and statical contributions in the production of Intermediate Mass Fragments (IMF) in semi-peripheral collisions was investigated through the CHI-FAR Experiment (see P. Russotto contribution in this volume). Performed in November 2019 at LNS, accelerating at 20 AMeV beams of ^{112,124}Sn and ^{124}Xe on ^{58,64}Ni and ^{64}Xe targets, the experiment aimed at extending the study of dynamical contributions to low bombarding energy. In semi-peripheral collisions, the emission of light IMFs emerging from prompt neck-fragmentation process and projectile-like fragments (PLFs) collinear massive breakup, characterized by timescales of tens of fm/c to 100 fm/c, is observed concurrently with equilibrated PLF binary fission-like emission, characterized by longer timescales. The presence of IMF dynamically emitted for the same systems was already investigated at 35 AMeV in the Reverse Experiment [8] and in the Inkissy experiment [9]. In a semi-peripheral reaction, a dynamical co-linear fission of one of the partners of the collision can occur, producing the lighter fragment of the two fissions fragments to be emitted toward the back of the fissioning system. This aligned fission is characterized by an anisotropy in the angular distributions. Indeed, the quasi projectile fission happens within the relaxation time, corresponding to very small proximity angles (*i.e.*, the angle θ_{PROX} (fig. 2, left panel) formed by the PLF velocity vector (along the TLF-PLF separation axis) and the velocity vector of the heaviest fragment between the two originating from the PLF decay), while statistical fission exhibits the isotropic distribution of θ_{PROX}. The previous Reverse experiment [8] highlighted that the dynamical component appeared to be favoured in the neutron rich system, while the Inkissy experiment [9] evidenced that the dynamical fission is ruled by the N/Z content of the projectile
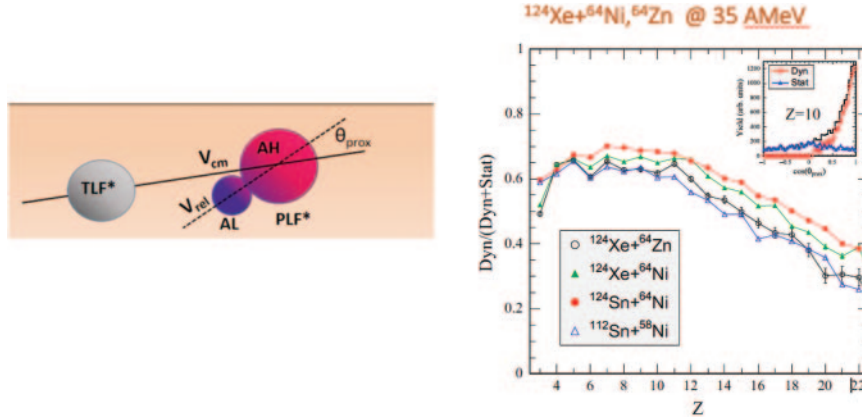
Fig. 2. – Sketch of the reference axes and θ_{PROX} as defined for a ternary event (left) and estimation of dynamical and statical contributions in the production of Intermediate Mass Fragments (IMF) in semi-peripheral collisions in the Inkissy Experiment [9].

and target, as illustrated in fig. 2 (right panel), and it is independent from the system size.

The more recent Chifar experiment extended these investigations to lower bombarding energies, using CHIMERA apparatus coupled with 10 telescopes of FARCOS Array. The FARCOS telescopes were arranged in a ring-like structure covering the angular polar range 16–30°. FARCOS (see E.V. Pagano contribution in this volume) allows studying LCP-LCP or IMF-IMF correlation functions, essential to get information on the space-time characteristics of the emission sources. The Acquisition system was implemented with the GET architecture for all the FARCOS signals [10, 11].

The presence of a less relaxed (or dynamical) component was analysed also at lower incident energies looking at the breakup of the projectile fragments in the peripheral collisions of the systems ^{78,86}Kr + ^{40,48}Ca at 10 AMeV [12, 13]. The reactions were investigated in the ISODEC experiment, aimed at the study of the isospin influence on reactions mechanisms and fragments production [14]. In particular, by analysing the relative emission angle of the two fission fragments, ascribable to the PLF breakup, it exhibited an important component at cosine $(\theta_{PROX}) = 1$, corresponding to an alignment of the two fission fragments with the separation axis of the PLF and TLF (lighter fragment emitted backward). These dynamical contributions are more important in the neutron rich system, in agreement with the results obtained in the Inkissy and Reverse Experiment at higher energies; in addition, an independence of the dynamical contribution from the asymmetry parameter A_H/A_L, defined as the ratio of the mass of heaviest fragment over the mass of lightest fragment, was observed.

The inspection of peripheral collisions at 35 AMeV also allowed proposing a new method for the estimation of the density in neck fragmentation processes (see A. Pagano talk and abstract contribution in this volume). Ternary reactions were selected and the two-particles relative kinetic energies of the three fragments emerging from the collision (IMF, PLF, TLF) were evaluated. The idea behind this method is that the effective size and density of the neck region, generating the IMF at the moment of full acceleration in the three-body splitting, could influence sharing the total kinetic energy decomposition. This method allowed estimating the neck density for ^{124}Sn + ^{64}Ni ternary reactions,
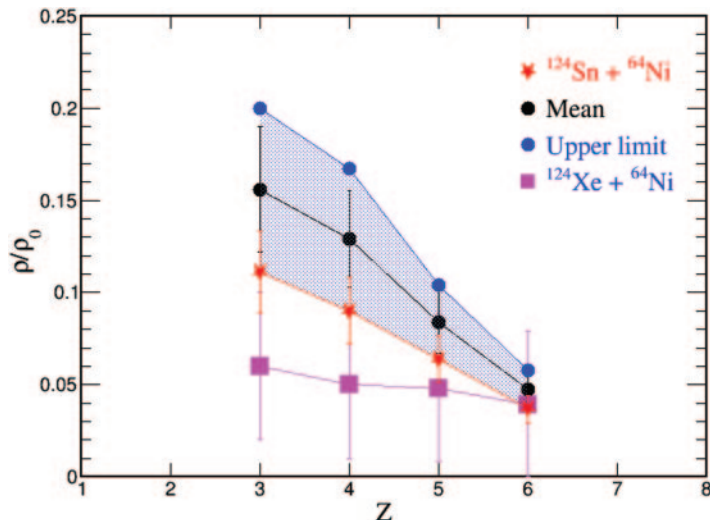
Fig. 3. – Extracted values of the relative density as a function of the IMF atomic number for ^{124}Sn$+^{64}$Ni (red points) and ^{124}Xe$+^{64}$Zn (cyan points) at 35 AMeV. The blue points represent an upper limit evaluation of the relative density including the systematic error (around 22%) contained in the method, while the black points are a mean value of the two sets (red and blue points) for the Sn + Ni system (from A. Pagano talk).

which resulted in the range 0.05–0.15 ρ/ρ_0 for IMF with charge $Z_{IMF} = 3$–6 [15]. These values, which are located at the lowest portion of the values present in literature [16], are in agreement with BNV predictions for the last stages of the expanding phase [17] and support the picture that neck-fragmentation, in agreement with transport model predictions, can be associated with a low-density expanding region located in the overlap zone between the projectile-like and target-like nuclei. The method was recently applied to the systems ^{112,124}Sn $+ {}^{58,64}$Ni and ^{124}Xe $+ {}^{64}$Zn,^{64}Ni to further check his sensitivity and dependence on N/Z of the entrance channels, and some of the obtained results are summarized in fig. 3.

The dynamics of Isospin equilibration in reactions involving the production of IMF in the mid-rapidity region is the focus of the EQUIL2 experiment. Accomplished at LNS in 2018, the experiment, performed accelerating at 40 AMeV ^{40,48}Ca beams on ^{27}Al and ^{40}Ca targets, aimed at studying the isospin equilibration process in different reaction mechanisms, in order to obtain information on crucial parameters of the symmetry energy of the nuclear equation of state, benefiting of CoMD model predictions [18, 19]. The investigation makes use of the measurements of the reduced value of the total dipolar signal, closely linked with the charge/mass equilibration process, obtained from the experimentally measured velocities and charges of all fragments produced in the collision [20], which can be directly compared with model predictions referring to different density functional-forms related to the symmetry energy.

4. – Study of central collisions at the onset of Fermi Energies

Analysis on experimental data collected in experiments performed some years ago produced results also for the study of reaction mechanisms involved in central collisions. In

particular, new results from the analysis of the ISODEC Experiment were obtained. The ISODEC experiment, which was proposed to investigate the competition of the different reaction mechanisms and their dependence on the N/Z of the entrance channel, used beams of ^{78,86}Kr, accelerated at 10 AMeV on ^{40,48}Ca targets [21]. Under the hypothesis of a complete fusion, which was confirmed for the 75% of the events, a compound nucleus was formed, with an excitation energy of almost 2 MeV per nucleon. A first analysis of the experiment allowed estimating the cross sections of the different reaction mechanisms, showing that the composite system formed in the fusion process between projectile and target leaves the place to an evaporation residue, produced through a long-lived system, which emitted light charged particles; however, most of the time the compound system would undergo fission processes [12-14]. The neutron poor system seems to present a slightly higher probability to populate the fusion-evaporation mechanism, while it has a strongly higher fusion-fission probability, showing globally more fusion than the neutron rich system. Recently, the thermal characteristics of the Evaporation Residue have been analysed (see B. Gnoffo contribution in this volume) by means of the construction of Albergo temperatures [22] (using He isotopes) and kinetic temperatures (extracted from the slope of the kinetic energy spectra) [23] for the fragments with $Z = 2$; the extracted double isotopic ratio temperatures exhibit values around 3–4 MeV, as commonly observed at the onset of the Fermi energies, while the slope temperatures, which do not show a dependence on laboratory emission angles, as expected in the case of emission by an equilibrated source, range in values typical of statistically evaporated particles. Both thermometric methods, *i.e.*, the chemical and kinetic methods, have shown an isospin influence on the temperatures, extracting a higher temperature for the neutron rich systems.

Recent results emerged also from the analysis of experimental data recorded in Thermo experiment, aimed at investigating the onset of Multifragmentation phenomenon and the thermodynamical characteristics of sources of a hundred nucleons at $E^{*} = 2$–4 AMeV, formed in central collisions, for the systems ^{58}Ni $+ {}^{40,48}$Ca at 25 AMeV. The central collisions were selected by imposing a selection on the variable Total Kinetic Energy (TKE ≤ 700 MeV), shown in fig. 4 (top right), isolating 10% of the well reconstructed events. At these bombarding energies, corresponding to the lower end of the Fermi energies, central collisions are dominated by events where a massive fragment, with a velocity close to the center of mass one, is emitted together with some light charged particles; in these reactions, an Evaporation Residue emerges in the final state, due to predominance of a one-body dissipation mechanism, the signature of mean-field behaviour. The total multiplicity of IMF (*i.e.*, fragments with $Z \geq 3$) displays a maximum peaked at $M_{IMF} = 2$–3 with a tail extending to $M_{IMF} = 5$–6 [24]. The events with $M \geq 4$ were associated to multifragmentation events. In order to confirm the onset of multifragmentation mechanism at this low energy, comparisons with the predictions of a dynamical approach based on the Boltzmann-Langevin-One-Body (BLOB) [25] were performed. After a first stage of pre-equilibrium emission, which leads the ^{58}Ni $+ {}^{40}$Ca system towards a value of N/Z of the emitting sources close to the stability valley while maintaining constant the N/Z of the emitting sources for the ^{58}Ni $+ {}^{48}$Ca system, Blob predictions for $b = 0$–3 fm mostly expect that a source of $A = 60$–70 amu and atomic number $Z = 30$ with an excitation energy of 2 AMeV is formed. In addition, about 25% of the events have a multiplicity of primary fragments equal two. The secondary sequential decay of these sources was simulated using the Gemini model on primary fragments at 300 fm/c. The charge distribution predicted by Blob + Gemini models (fig. 4, top left) roughly recalls the shape of the experimental distribution associated to events with
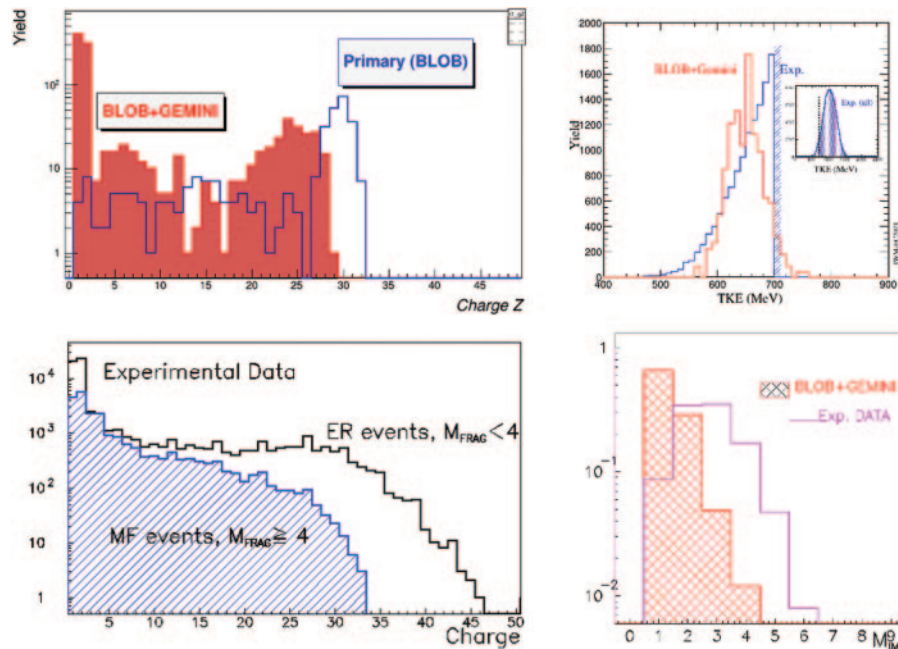
Fig. 4. – Central Collisions for ^{58}Ni$+^{40}$Ca at 25 AMeV: charge distributions of primary (BLOB) and final fragments (BLOB + GEMINI) for $b = 0$–3 fm collisions (top left panel) and the experimental one (bottom left panel); the TKE used to select the centrality of the collisions for simulated and experimental data (top right) and the simulated and experimental IMF multiplicity distribution (bottom right).

$M_{IMF} < 4$ (fig. 4, bottom left), where the presence of a very massive fragment can be associated to an Evaporation Residue (ER) formation pattern. On the other hand, the range of the BLOB + Gemini charge distribution is closer to the experimental distribution obtained for the multifragmenting sources, characterized by $M \geq 4$; in addition, even if the theoretical IMF multiplicity distribution is still characterized by a lower IMF average production than the experimental one (fig. 4, bottom right), simulations of the decay of an evaporation residue, as predicted by BLOB, are not able to reproduce the experimental IMF multiplicity values. Correlations of the charges of the three biggest fragments can be useful tools to investigate the character of the IMF emission and further investigations are in progress.

5. – Investigating population and gamma-ray decay of ^{12}C levels

Confident in the capability of CHIMERA CsI(Tl) to detect gamma rays with a modest energy resolution but with a satisfactory efficiency, granted by the 4π coverage, and the uniqueness of the simultaneous efficiency detection of charged particles [26], we tried to contribute to the lively debate on the Hoyle state of ^{12}C [27] (see G. Cardella contribution in this volume).

The decay of ^{12}C levels above the particle emission threshold plays a crucial role in the production of ^{12}C in astrophysical environments. The Hoyle state (7.65 MeV) is fundamental in the helium burning phase of red giant stars, while the 9.64 MeV level can be involved in higher temperature explosive environments.

The gamma decay of the excited ^{12}C was studied by analysing the reaction products of ^{4}He + ^{12}C at 64 MeV and $p + {}^{12}$C at 24 MeV systems, employing the complete redundant method, which imposes the simultaneous detection of scattered alpha (or proton) projectile, carbon target and the two gammas (corresponding to a two-steps decay from ^{12}C*) in order to efficiently reduce the background [28]. The values obtained for the Hoyle state gamma decay width are higher than the ones presented in literature, obtained with more precise measurements of gamma energies [29]; however, also a recent result [30] extracted a larger value for the gamma decay width. In addition, the decay from 9.64 MeV level was observed, which was rarely measured before [31]. The analysis of the Hoyle2 experiment, performed in June 2020, will be used to improve the statistics of the present analysis. In addition, a detailed investigation on a possible population of an Efimov State at 7.46 MeV was recently performed [32]. The research is in progress. However, a first observation seems to exclude the presence of a sequential decay of this state, while our data could be compatible with its direct decay.

6. – Planning new investigations

Due to the restrictions imposed by the pandemic, some of the experiments planned in 2020 were postponed until resumption of the accelerator activities. Indeed, in September 2020, the LNS accelerators were stopped to allow for the expansion of the construction work of the POTLNS project. The project aims at the production of high intensity ion beams by upgrading the existing and operating devices, designed for the fundamental research in Nuclear Physics. Upgrading the Superconductive Cyclotron (CS) will provide stable ion beams with a power up to 10 KW, for ions from Carbon to Argon with intensities up to 10^{13}–10^{14} pps (see N. Martorana contribution in this volume). This will allow producing unstable ion beams thanks to the FRAISE facility [33, 34], with an intensity up to 10^3–10^7 pps, using the in-flight fragmentation method. FRAISE will make possible to deliver neutron-rich and neutron-poor nuclei also to CHIMERA reaction chamber, allowing extending the study of isospin dependence in heavy ion reactions at Fermi energies to more extreme values of isospin asymmetries. The end of the construction work is planned for Winter 2023 and the Tandem should start to be operative again in Spring 2023, while the CS will be switched on again for preparation and testing in Fall 2023. New efforts, endorsed also with an important financial support assigned by the Italian Ministry of Research after a very selective competition (PRIN2020), are devoted to design a compact and versatile array, able to detect the neutron signal and charged light particles simultaneously [35]. The design phase will also benefit from the expertise gained with FARCOS: the 20 telescopes are completed and 10 of them were used in the final configuration in CHIFAR experiment, giving promising first results (see E. V. Pagano contribution in this volume).

7. – Conclusions

Several activities are expected for the next years. The LNS-CS upgrade will give high intensity stable beams, thanks to the accomplishment of the POTLNS project. The experimental activities are expected to resume as soon as the construction site will be closed and testing the new beam lines and operational functions of the accelerators will be the first actions to be performed. The FRAISE facility will open new explorations providing a wide range of radioactive beams at high intensity. Interesting analyses for semi-peripheral collisions from 10 to 40 AMeV are studying the presence of dynamical

components in the PLF Break-up, in system with different sizes; at the same time, central collisions for $E_{BEAM} = 10\text{–}40$ AMeV are analysed to assess isospin influence and equilibration in reaction mechanisms and to study thermodynamical features of the formed sources. The activities connected with the collaboration R3B (Reaction with Relativistic Radioactive beam) at GSI are continuing, in order to extend the topics typically studied by our collaboration (fission, clustering, symmetry energy, etc.) to relativistic energies and to explore the equation of state of nuclear matter at high densities. Efforts to include neutron detection in our devices are going on, supported by promising results.

* * *

REFERENCES

[1] Russotto P. *et al.*, *Phys. Rev. C*, **94** (2016) 034608.
[2] Li Q. *et al.*, *J. Phys. G*, **31** (2005) 1359; **32** (2006) 407.
[3] Russotto P., Le Fèvre A., Lukasik J. *et al.*, arXiv:2105.09233 (2021).
[4] Lukasik J. *et al.*, *Nuovo Cimento C*, **41** (2018) 182.
[5] Boretzky K., Gašparić I. *et al.*, *Nucl. Instrum. Methods A*, **1014** (2021) 165701.
[6] Pagano E. V. *et al.*, *EPJ Web of Conferences*, **117** (2016) 10008.
[7] https://www.r3b-nustar.de/.
[8] Russotto P., De Filippo E., Pagano A. *et al.*, *Phys. Rev. C*, **91** (2015) 014610.
[9] Russotto P., De Filippo E., Pagano E. V. *et al.*, *Eur. Phys. J.*, **56** (2020) 12.
[10] Pollacco E. *et al.*, *Nucl. Instrum. Methods A*, **887** (2018) 81.
[11] De Filippo E. *et al.*, *J. Phys.: Conf. Ser.*, **1014** (2018) 012003.
[12] Gnoffo B. *et al.*, *Nuovo Cimento C*, **41** (2018) 177.
[13] Pirrone S. *et al.*, *EPJ Web of Conferences*, **223** (2019) 01051.
[14] Pirrone S., Politi G., Gnoffo B. *et al.*, *Eur. Phys. J. A*, **55** (2019) 22.
[15] Pagano A., De Filippo E. *et al.*, *Eur. Phys. J. A*, **56** (2020) 102.
[16] Wada R. *et al.*, *Phys. Rev. C*, **85** (2012) 064618; Liu X. *et al.*, *Nucl. Phys. A*, **933** (2015) 290.
[17] Baran V., Colonna M., Di Toro M. *et al.*, *Nucl. Phys. A*, **730** (2004) 329.
[18] Papa M. *et al.*, *Phys. Rev. C*, **64** (2001) 024612.
[19] Papa M. *et al.*, *Phys. Rev. C*, **87** (2013) 014001.
[20] Papa M. *et al.*, *Phys. Rev. C*, **91** (2015) 041601R; Papa M. *et al.*, *J. Phys.: Conf. Ser.*, **1643** (2020) 012103.
[21] Pirrone S. *et al.*, *J. Phys.: Conf. Ser.*, **515** (2014) 012018.
[22] Albergo S. *et al.*, *Nuovo Cimento A*, **89** (1985) 1.
[23] Weisskopf V. F. *et al.*, *Phys. Rev. C*, **52** (1937) 295.
[24] Geraci E. *et al.*, *J. Phys.: Conf. Ser.*, **1643** (2020) 012087.
[25] Colonna M. and Napolitani P., *Phys. Rev. C*, **96** (2017) 054609.
[26] Cardella G. *et al.*, *Nucl. Instrum. Methods A*, **799** (2015) 64.
[27] Freer M. and Fynbo H., *Prog. Part. Nucl. Phys.*, **78** (2014) 1.
[28] Cardella G. *et al.*, *Phys. Rev. C*, **104** (2021) 064315.
[29] Hoyle F., *Astrophys. J. Suppl. Ser.*, **1** (1954) 121.
[30] Kibeti T. *et al.*, *Phys. Rev. Lett.*, **125** (2020) 182701.
[31] Tsumura M. *et al.*, *Phys. Lett. B*, **817** (2021) 136283.
[32] Cardella G. *et al.*, *Nucl. Phys. A*, **1020** (2022) 122395.
[33] Russotto P. *et al.*, *J. Phys.: Conf. Ser.*, **1014** (2018) 012016.
[34] Martorana N. S. *et al.*, *Nuovo Cimento C*, **44** (2021) 1.
[35] Pagano E. V. *et al.*, *Nucl. Instrum. Methods A*, **889** (2018) 83.